Mean Flow Characteristics for the Oblique Impingement of an Axisymmetric Jet

J.F. Foss*
Michigan State University, East Lansing, Mich.
and
S.J. Kleis†
University of Houston, Houston, Texas

Theme

THE oblique impingement of an axisymmetric jet on a large plane surface was the subject flow for the investigation reported herein. Figure 1 presents a schematic representation of the flowfield, and defines the variables used for its description. This study was motivated by the "under the wing, externally blown flap" configuration for STOL aircraft; its objectives were to identify the characteristics of this flowfield and to infer the dominant mechanisms responsible for them. If the propulsion jet interacts with the airfoil surface prior to its impingement upon the extended flap, then the proper design of the gap should allow the streamwise vorticity, which is created by the interaction, to be passed to the suction side of the flap. The geometric range of experimental interest, $0.5 < h/d \leq 2$, $0 \leq x/d \leq 5$, and $0 < \alpha \lesssim 12°$ was suggested by this motivation problem. A large number of α and h/d values were examined; however, only experimental data for $\alpha = 9$; $h/d = 1$ are presented herein. The complete set of results is given in Ref. 1; an abridged set is provided in the reference manuscript.

Previous literature references on the shallow angle, oblique jet impingement flowfield have not provided for its extensive documentation. A discussion of the relevant literature is given by the authors in the reference manuscript.

Contents

The flow system was designed such that the jet could be formed from either a fully developed pipe flow or a relatively short nozzle with a rather uniform mean velocity profile. A large plate, hinged to provide variable angles α and movable in the lateral direction, served as the plane-wall. Calibration information for the 4 linearized wires was first stored in the computer and then used for the subsequent computation of the velocity; hence, the accuracy of the u/u_0 data is only limited by the pressure transducer used for the calibration ($\simeq 0.5$ fps, $15 \lesssim \mu \lesssim 120$ fps), and the pitch/yaw effects associated with the flow at the location of the vertical hot-wire probe. The position of the probe was controlled by the computer via stepping motor drives.

The presence of the plate imposes a kinematic, no penetration, constraint on the behavior of the jet. The response of the jet fluid will be to spread horizontally and/or to deflect vertically with respect to the horizontal plate. The balance between these two effects is dictated by the dynamics of the interaction and is inferred from a comparison of the deflected/undeflected jet width measures. The undeflected width is provided by the intersection of the surface $u(x,r) = 0.1\ u_0$ and the plane of the plate. A cone, of half angle 5.7° and 4° for the fully developed and uniform cases, respectively, quite adequately describes the jet surface for $0 \leq x/d \leq 5$.

The contours of constant pressure in the plane of the plate suggested an appropriate measure of the jet spread (see Fig. 2). This figure includes both the reference curve and the static pressure contours, and indicates that there is little systematic spreading for $\alpha = 9°$, $h/d = 1$; this result is general for the shallow angle cases. The reference curve width is approximately 70 % that of the zero isobar contour at the x location of maximum pressure, and a nominal value of 0.3 describes the isobar which aligns with this reference curve. This result is some what general for the shallow angle cases.

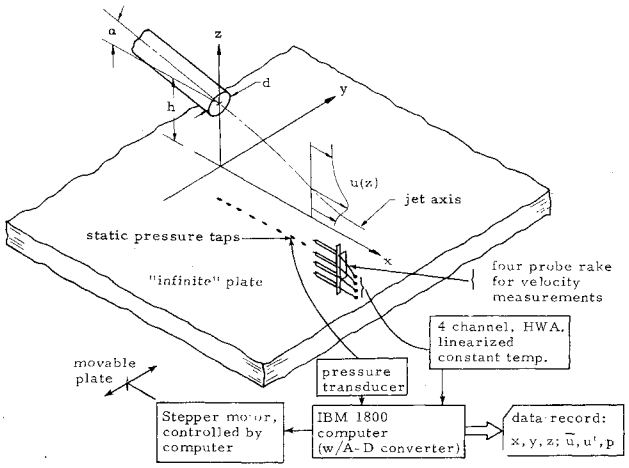

Fig. 1 Schematic of flowfield, experimental facility, and coordinate system.

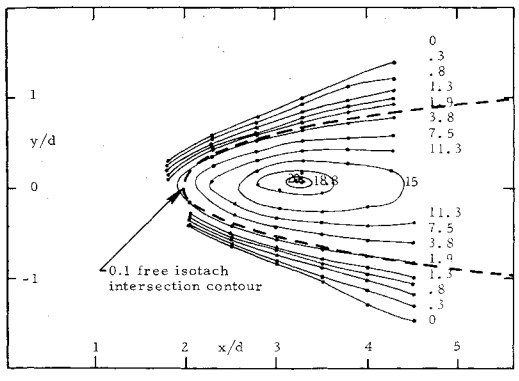

Fig. 2 Surface isobars for the conditions $\alpha = 9$ degrees, $h/d = 1$, "uniform flow" nozzle. Values shown are $p(x,y,0)/\rho u(o)^2 \lambda \sin \alpha$ where λ = momentum flux correction factor ($= 0.809$).

Received Aug. 4, 1975; synoptic received Nov. 14, 1975; revision received March 23, 1976. Full paper available from National Technical Information Service, Springfield, Va., 22151, as N/6-21425 at the standard price (available upon request). Research supported by NASA Lewis Research Center, NGR 23-004-068. The assistance of D.Yen, Michigan State University, Dept. of Mathematics, in the stagnation point analysis is gratefully acknowledged.

Index categories: Jets, Wakes, and Viscid-Inviscid Flow Interactions.

*Professor, Department of Mechanical Engineering. Member AIAA

†Presently, Assistant Professor, Department of Mechanical Engineering, formerly, Graduate Assistant, Division of Engineering Research, Michigan State University.

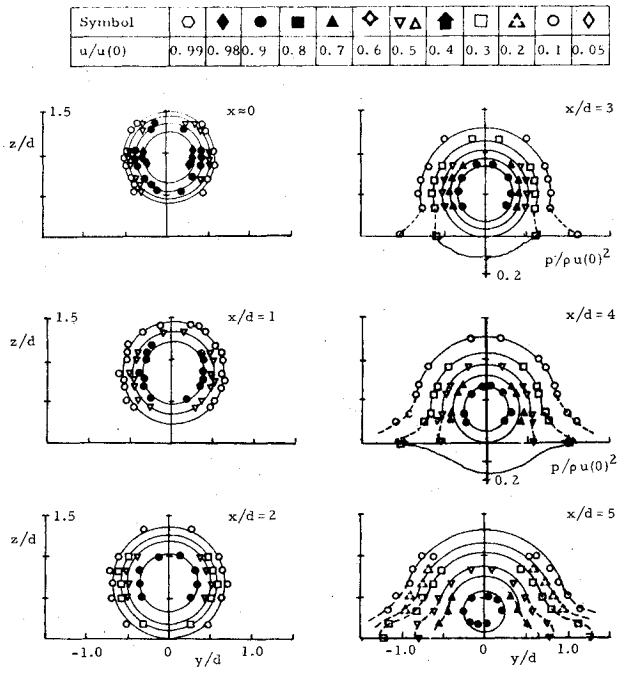

Fig. 3 Isotach distributions. (Contours shown are level surfaces of $\bar{u}(y,z)/u(o)$ for a given x location.

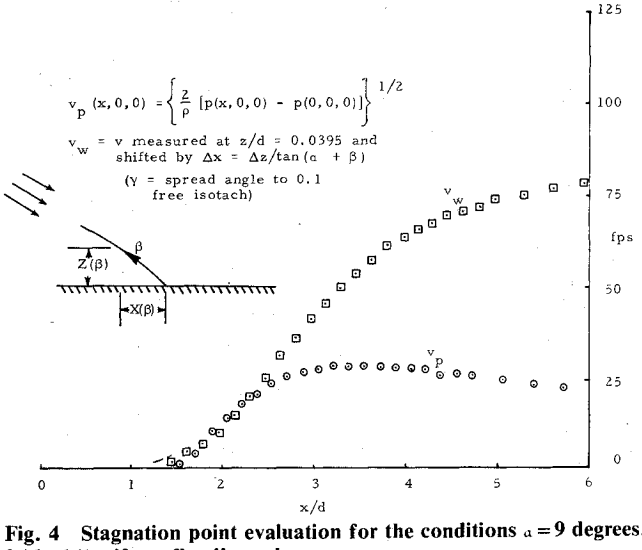

Fig. 4 Stagnation point evaluation for the conditions $\alpha = 9$ degrees, $h/d = 1$ "uniform flow" nozzle.

The static pressure contours define the "dynamic" jet width. Alternatively, the velocity field data can be used to infer a "kinematic" jet width (see Fig. 3). The lateral pressure distributions at the same longitudinal locations clearly show that the kinematic width is substantially larger than the dynamic width. For example, the isotach contours which correspond with the "zero" pressure location, namely $u/u_0 = 0.1$, 0.3, and 0.5 for $\alpha = 3°$, 9°, and 15° respectively, demonstrate this.

The isotachs also reveal an important feature of the streamwise vorticity field. Specifically, the surface flux of $\pm\omega_x$, which is caused by the pressure gradients $\pm|\partial p/\partial y|$ on the $\mp y$ sides of the jet, respectively, results in the bulging skirts of the isotachs. Analytically, the surface pressure gradients are related to the volume integral of the vorticity transport equations through the viscous diffusion terms; i.e.,

$$\int_{\text{c.s.}} \nu(\partial\omega_i/\partial x_j)\, n_j dA \cong \int_{A_P} \hat{i}(\partial p/\rho\partial y - \hat{j}\partial p/\rho\partial x - \hat{k}\partial\omega_z\partial z)\, dA,$$

where c.s. is the control surface, and A_p is the area of the plate

$$\int_{\text{c.s.}} \omega_x (u\cdot\hat{n})\, dA = \int_{\text{c.v.}} \omega\cdot\nabla u dV + \int_{A_P} \frac{1}{\rho}\frac{\partial p}{\partial y} dA \qquad (1)$$

for a control surface extending from the jet exit to the downstream plane of interest and bounded by the impact plate, the plane $y = 0$ and a surface, in the entrainment flow, which closes the control volume.

On a gross scale, the jet flow impacts upon the plate, deflects vertically, and/or spreads laterally as noted above; more precisely, only the stagnation streamline‡ impacts upon the plate. The analysis which related the orientation of the stagnation streamline to the characteristics of the flow is presented in the reference manuscript. The orientation of the stagnation streamline is, (see Fig. 4 for the definition of terms),

$$\frac{dZ}{dX}(0) = -\frac{3\mu(\partial\omega_y/\partial x)_{z=0}}{\partial p/\partial x} \equiv \xi'(0) \qquad (2)$$

and this result can be used to infer that the stagnation point can be located in a region of adverse pressure gradient or at a pressure maxima since $0 > \xi'(0) \gtrsim -\infty$ and $(\partial\omega_y/\partial x) > 0$, $\partial p/\partial x \geq 0$.

The experimental technique to identify the stagnation point makes use of a velocity magnitude measurement at $(x,\delta z)$, and a static pressure measurement at $(x,0)$. It is based upon the equivalence of the stagnation pressure at $z = 0$ and a small δz value above the plate; i.e., δz is assumed small enough ($\delta z/d \simeq 0.04$) that the alteration of the stagnation pressure resulting from shear effects is negligible. The technique also assumes that the δz value is sufficiently large such that the static pressure is essentially equal to the atmospheric value. (A violation of the second assumption means that the true stagnation point is farther upstream than the technique suggests.) For convenience of representation, the surface static pressures were converted to an equivalent "stagnation streamline" velocity v_p; that is,

$$v_p(x) = \{2[p(x,0,0) - p_{\text{atm}}]/\rho\}^{1/2} \qquad (3)$$

A Disa gold-plated probe (to reduce pitch effects) was traversed at $y = 0$, and $z = \delta z$, and the velocity v_w was recorded and transferred to the location of the plate along ray. This accounted for the inclination angle (α) and the divergence angle of the 0.1 isotach (γ); viz., v_w $(x,\delta z)$ was shifted by an amount δx where

$$\delta x = \delta x \tan^{-1}(\alpha + \gamma) \qquad (4)$$

The stagnation point is considered to be the point of tangency between the $v_w(x)$ and $v_p(x)$ curves.

The experimental data for $\alpha = 9°$, $h/d = 1$ are presented in Fig. 4. Significantly, the indicated stagnation points: $x_s/d \simeq$ 3.8. 1.9, 1.3 for the conditions: uniform nozzle, $h/d = 1$ and $\alpha = 3°$, 9°, 15° respectively, are close to the intersections of the 0.1 isotachs with the plane of the plate. As noted earlier, the overlapping $v_w(x)$ and $v_p(x)$ curves suggest the possibility of a finite length stagnation line (i.e., the curves appear to be tangent over a region).

References

[1] Foss, J.F. and Kleis, S.J. "The Oblique Impingement of an Axisymmetric Jet," Second Annual Report, NASA Lewis Research Center, NGR 23-004-068, Dec. 1972.

‡Time averaged quantities are exlusively considered in this section. The stagnation streamline is defined as the locus of points everywhere tangent to the velocity field with a terminus (the stagnation point) on the impact plate. The presence of a finite length stagnation line will be suggested by the experimental data, and it cannot be excluded by analytical cosiderations. However, the general discussion and the analysis will implicity assume a single stagnation streamline.